Simulation of 2D fields of raindrop size distributions

A. Berne[1], M. Schleiss[1] and R. Uijlenhoet[2]
(1) EPFL-LTE, Lausanne, Switzerland. (2) HWM, Wageningen, The Netherlands

I. Introduction

Quantitative applications of weather radar measurements require accurate and reliable rain rate estimates. For the conversion of measured radar reflectivities into rain rates, the raindrop size distribution (DSD in the following) plays a major role, as the parameters used in the Z-R relationship depend on the size and concentration of hydrometeors in the considered radar sampling volume (e.g., [1], [2]). In addition, the shape (which is related to the size) is also relevant for the quantitative interpretation of polarimetric radar measurements [3]. Hence, the variability of the DSD in space and time has to be taken into account to improve radar rain rate estimates.

Different simulation frameworks have been proposed and used to investigate many issues related to weather radar measurements (e.g., [4]–[6]). The ability to generate a large number of 2D fields of DSDs which are statistically homogeneous provides a very useful simulation framework that can be used to obtain reliable statistical characterizations of a variety of issues related to radar beam propagation through rain as well as radar retrieval techniques. Such a framework nicely complements experimental approaches based on DSD data in order to investigate radar rain rate estimation.

In the present paper, a stochastic simulator with such an ability is proposed. It is based on a previously developed 1D simulator [7]. Section II describes the proposed 2D simulator. The data set used to parameterize the simulator is presented in Section III. In Section IV, examples of generated fields are presented; in particular simulated radar reflectivity fields are compared to observed ones to assess the quality of the simulations. Finally some conclusions are given in the last section.

II. Modelling the spatial variability of the DSD

Raindrop size distributions are highly variable in space and time over a large range of scales because of the variability of microphysical processes and atmospheric turbulence [8]. In the present paper, we will focus on rainfall at the ground level or closeby, hence limiting our investigation to 2D fields of liquid rain. In this framework and for a given area at a given time, DSD values can be seen as a realization of a random function with a spatial and temporal structure (e.g., [9]).

In a previous study, we proposed a stochastic simulator to generate 1D range (or time) profiles of DSDs [7]. This simulator has been applied to investigate different aspects of radar retrieval ([7], [10]–[12]). The DSD simulator is based on two main assumptions.

First, the DSD is assumed to be adequately described by an exponential model:

$$N(D|N_t,\Lambda) = \alpha N_t e^{-\Lambda D} \tag{1}$$

where N_t [$\mathrm{m^{-3}mm^{-1}}$] denotes the concentration of drops and Λ [$\mathrm{mm^{-1}}$] the exponential slope; α [$\mathrm{mm^{-1}}$] is a normalization factor introduced because of the finite range of diameter values between D_{min} and D_{max}, depending on Λ:

$$\alpha = \frac{1}{\int_{D_{min}}^{D_{max}} e^{-\Lambda D}\, dD} \tag{2}$$

N_t and Λ are supposed to be random variables that are jointly lognormally distributed.

Second, the correlation structure is assumed to be correctly described using a vector autoregressive process of order 1 (which implies an exponential autocorrelation function). The spatial correlation is characterized by its scale of fluctuation [13]. For more details, the reader is referred to [7].

The objective of the present paper is to extend this 1D simulation framework in 2D. We keep the basic assumption of an exponential DSD and a jointly lognormal distribution of the two parameters N_t and Λ. A difficulty arises concerning the spatial structure of the simulated fields in 2D. Autoregressive processes cannot be easily and satisfactorily extended in 2D because it is difficult to simulate a given correlation structure (especially isotropic ones, e.g., [14]). Moreover, only a limited range of functional forms for the spatial structure can be simulated using autoregressive processes (see [13], p.124). Therefore we have to implement another approach in order to simulate realistic DSD fields in 2D.

Geostatistics have been developed to provide a theoretical framework for the analysis of spatially correlated random fields (e.g., [15]). The spatial structure is characterized by the semi-variogram (designated as variogram in the following) of a random function F:

$$\gamma(h) = \frac{1}{2}\mathrm{E}\left\{\left[F(\mathbf{x}+\mathbf{h}) - F(\mathbf{x})\right]^2\right\} \tag{3}$$

where E denotes the expectation, $\mathbf{x}$ is a position vector (in 2D in the present paper) and $\mathbf{h}$ is a separation vector. In order for the variogram to be defined, F must be a second order intrinsic random function (i.e., its increments are second order stationary, see [15]). This assumption is less restrictive than the second order stationarity (i.e., the random function itself is second order stationary).

As previously mentioned, we assume an exponential DSD with 2 parameters that are lognormally distributed. Hence multivariate geostatistics will be used. Taking advantage of the fact that Gaussian random fields are easier to simulate, F is defined as

$$F(x) = \begin{bmatrix} \ln[N_t(\mathbf{x})] \\ \ln[\Lambda(\mathbf{x})] \end{bmatrix} \tag{4}$$

To simulate 2D fields of $\ln N_t$ and $\ln \Lambda$ values, the necessary information is the mean and the standard deviation, as well as the variogram and cross-variogram of both $\ln N_t$ and $\ln \Lambda$. These (cross-)variograms can take into account the possible anisotropy of rainfall. The package gstat [16] of the R software is used to perform such 2D Gaussian simulations. 2D fields of N_t and Λ values (therefore of DSDs) are obtained by exponentiating the simulated Gaussian 2D fields of $\ln N_t$ and $\ln \Lambda$. It must be noted that the proposed approach only generates strictly positive rainfall and hence cannot produce intermittent rainfall fields. The parameterization of the algorithm is described in the next section.

III. Parameterization and data set

In order to rigorously derive the parameters of the 1D or 2D models described in the previous section, it is necessary to have measurements of DSDs over a 1D or 2D spatial domain. However, such data are not available (with spatial resolutions adequate for the estimation of the spatial structure). DSD data are generally available as time series. Following the approach used by [7], DSD times series can be converted into range profiles of DSDs assuming Taylor's hypothesis. In order to extend the spatial structure estimated from 1D profiles to 2D fields, we have to further assume that the considered rainfall fields are isotropic. In the present paper, the parameters of the 2D simulator (i.e., mean and standard deviation for both $\ln N_t$ and $\ln \Lambda$, as well as the corresponding variograms) will be derived from a data set representative of intense Mediterranean rainfall.

This data set was collected using an optical disdrometer during the HIRE'98 experiment that took place during the autumn 1998 in Marseille, France [17]. We focus on a period of 45 min of intense rainfall (total amount of about 32 mm with an average rain rate of about 42 mm h^{-1}) during the 7 September 1998 rain event in order to simulate high rainfall intensities. To convert the measured DSD time series to DSD range profiles, we assume Taylor's hypothesis with a constant velocity of 12.5 m s^{-1} [18]. A temporal resolution of 20 s corresponding to 250 m in space has been selected in order to be able to simulate domains of about 30×30 km^2 with reasonable computation time. An exponential model is then fitted on the observed profiles of DSD spectra to derive range profiles of $\ln N_t$ and $\ln \Lambda$ values. The empirical distributions of $\ln N_t$ and $\ln \Lambda$ are given in Figure 1. The assumption of normality for $\ln N_t$ and $\ln \Lambda$ appears reasonable, despite the slight asymmetry of the distributions.

In addition, Figure 2 displays the sampling (cross-)variograms of $\ln N_t$ and $\ln \Lambda$. A variogram model with the required mathematical properties (see [15]) must be fitted on the sampling variogram that usually does not have the desired properties. In the present case, the variograms of $\ln N_t$ and $\ln \Lambda$ exhibit complex structures that will be modelled as nested structures. Hence a sum of 2 spherical variogram models is fitted on each sampling variogram:

$$\gamma(h) = \gamma_{sph,1}(h) + \gamma_{sph,2}(h) \tag{5}$$

with

$$\gamma_{sph,i}(h) = \begin{cases} C_{0,i} + C_{1,i}\left(\frac{3}{2}\frac{h}{a_i} - \frac{1}{2}\frac{h^3}{a_i^3}\right) & h < a_i \quad i = 1,2 \\ C_{0,i} + C_{1,i} & h \geq a_i \quad i = 1,2 \end{cases} \tag{6}$$

where C_0 denotes the nugget, $C_0 + C_1$ denotes the sill of the variogram, h the interdistance (direction is not relevant as we assume isotropy) and a the range. The total variance of the random function corresponds to the sum of the two partial sills and the nugget. The fitted parameter values are listed in Table I. The nugget effect (which results from the addition of possible sub-scale variability and measurement errors) is negligible for $\ln \Lambda$ but significant for $\ln N_t$. The first range is similar for $\ln N_t$ and $\ln \Lambda$ (about 2 km) while the second range is significantly larger for $\ln \Lambda$ (17 vs. 10 km). The cross-variogram indicates a weak correlation between $\ln N_t$ and $\ln \Lambda$ and they will be considered as independent in the following. The fitted variogram model is then simply $\gamma_{\ln N_t, \ln \Lambda} = 0$. It must be noted that this is suggested by the data but not a requirement of the proposed approach. These fitted variogram models will be used to generate 2D fields of $\ln N_t$ and $\ln \Lambda$ values, and subsequently 2D fields of DSDs, with the same spatial structure.

TABLE I
Nugget, range (in km) and sill of the exponential models fitted on the sampling variograms of $\ln N_t$ and $\ln \Lambda$.

	Nugget	Range 1	Range 2	Sill 1	Sill 2
$\ln N_t$	0.060	2.1	10.0	0.205	0.153
$\ln \Lambda$	0.002	1.7	17.0	0.043	0.075

IV. Simulation of 2D fields of DSDs

Applying the approach described in the previous sections, we are able to generate as many as desired 2D fields of DSDs that exhibit the same statistical properties. Figure 3 shows one simulated field of N_t and Λ values. Because the parameterization is established using 1D (time) DSD measurements, the simulated fields are isotropic. It must be noted that the proposed framework can generate anisotropic fields if relevant parameter values are provided.

From DSD values, bulk variables characterizing rainfall (e.g., radar reflectivity, rain rate, liquid water content) can be easily derived. During HIRE'98, measurements from an operational S-band (about 10 cm walength) weather radar located at about 100 km from Marseille were also collected. Reflectivity measurements over a 32×32 km^2 area with a 1-km^2 resolution over Marseille have been extracted. The considered period corresponds to 8 time steps of the operational radar (5 min time resolution).

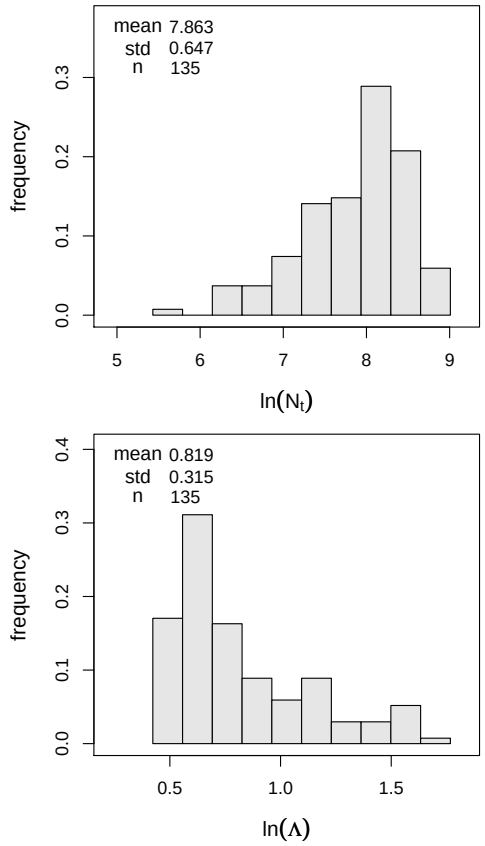

Fig. 1. Empirical distributions of $\ln N_t$ (top) and $\ln \Lambda$ (bottom) values estimated from intense Mediterranean DSD measurements.

In order to evaluate the quality of the simulation framework, the simulated 2D fields of DSD are converted into radar reflectivity fields using Mie theory [19], averaged at a 1-km^2 resolution and then compared to the observed radar reflectivity fields.

The comparison is first performed on the basic statistics: mean and standard deviation. Because the simulator is not able to reproduce intermittency, the comparison will be limited to values above a given threshold. Due to quantization effects in the measured reflectivity values, the threshold is fixed at 20 dBZ. Figure 4 presents the distribution (for 500 simulations) of the mean value of the simulated reflectivity (expressed in dBZ) as well as the corresponding range of observed mean values. The simulated and observed distributions are consistent with a slight overestimation in the order of 2 dBZ. Figure 5 is similar to Figure 4 but for the standard deviation. The agreement between simulated and observed values is even better for the standard deviation.

Next, the simulated and observed spatial structures of the reflectivity fields are compared in order to assess the consistency of the simulation with measurements. Figure 6 shows a variogram representative of the simulated reflectivity fields together with the minimum and maximum variograms of the observed reflectivity fields. Although not identical, these variograms are in very good agreement with each other, indicating

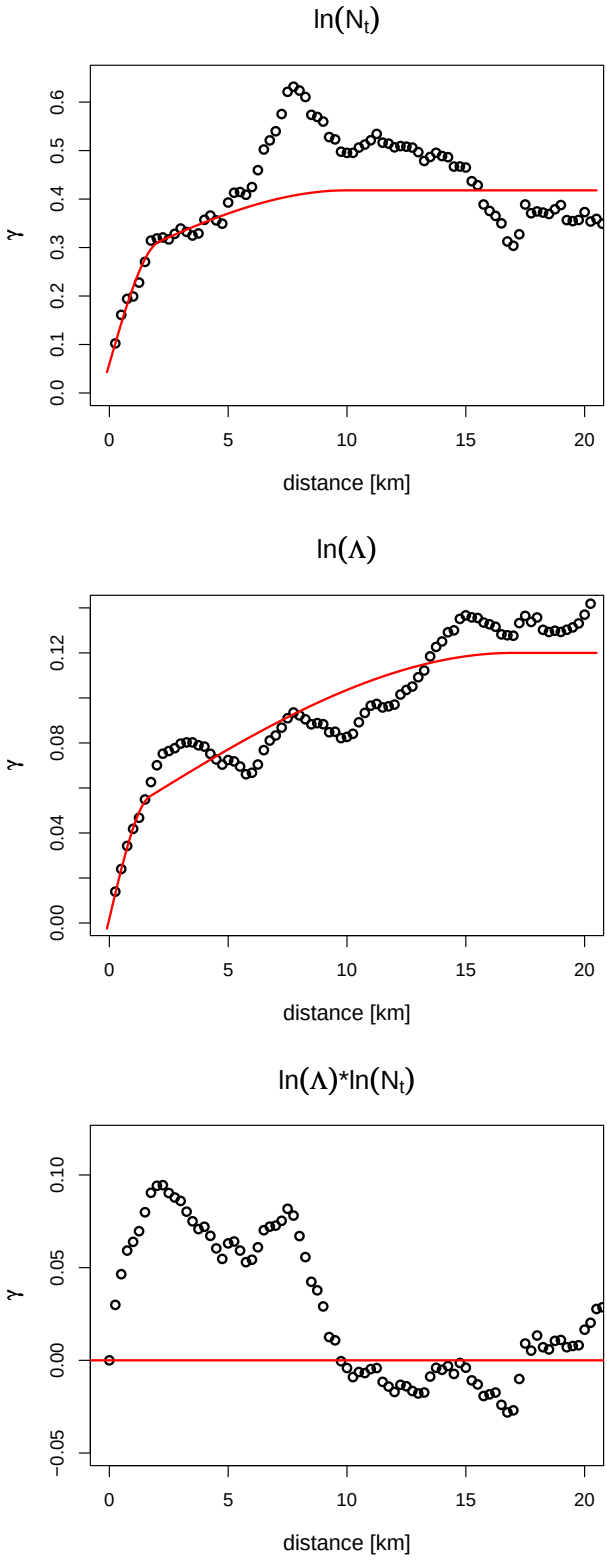

Fig. 2. Variogram of $\ln N_t$ (top), variogram of $\ln \Lambda$ (middle) and cross-variogram (bottom) estimated from intense Mediterranean DSD measurements. The solid red lines represent the fitted variogram models.

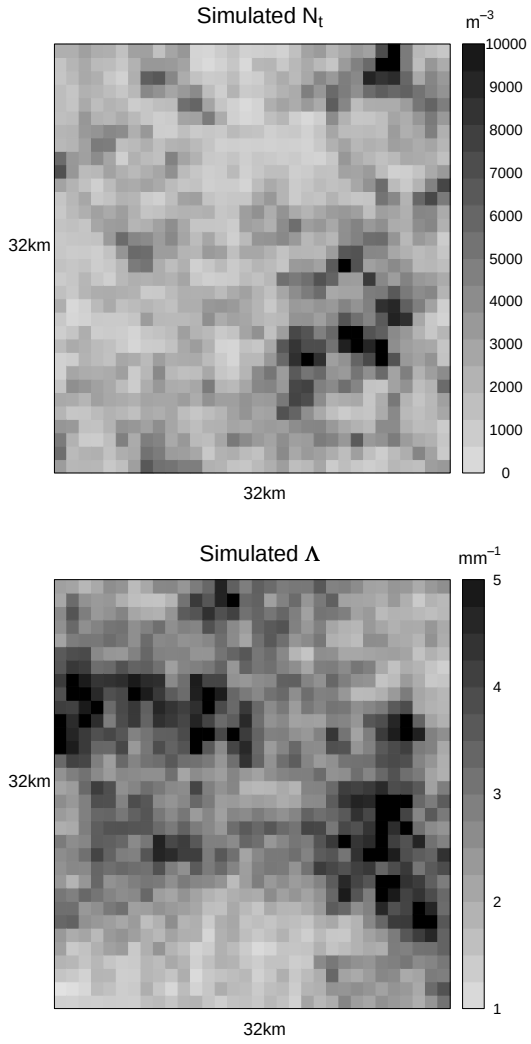

Fig. 3. Simulated fields of N_t (top) and Λ (bottom) values with the spatial structure corresponding to the fitted variogram models given in Figure 2.

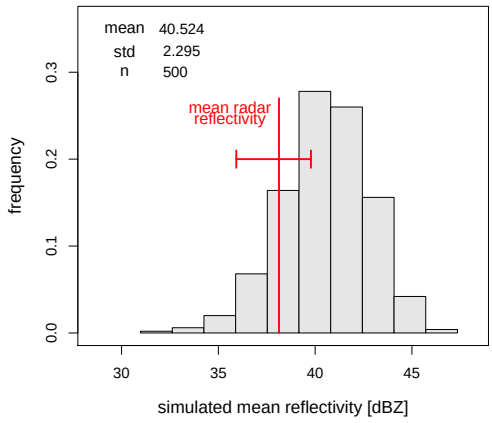

Fig. 4. Distribution of the mean values of the simulated fields of radar reflectivity (in dBZ). The red line figures the average of observed mean values and the associated horizontal bar indicates the min and max observed values.

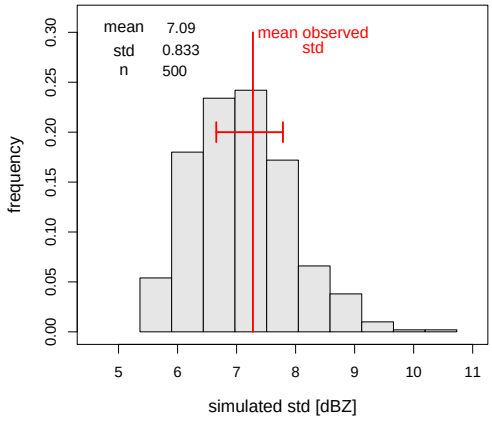

Fig. 5. Distribution of the standard deviation values of the simulated fields of radar reflectivity (in dBZ). The red line figures the average of observed standard deviation values and the associated horizontal bar indicates the min and max observed values.

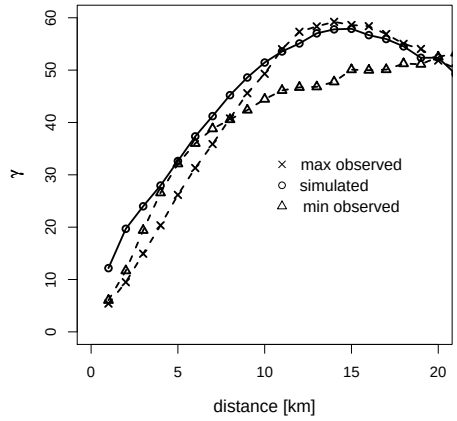

Fig. 6. Simulated (circles), observed minimum (triangles) and observed maximum (crosses) variograms of reflectivity values (in dBZ) over a 32×32 km^2 domain with a 1-km^2 resolution.

that the generated fields have the appropriate spatial structure. This together with the fact that the statistics of the observed reflectivity fields are correctly reproduced demonstrate the ability of the proposed simulator to generate realistic 2D fields of DSDs.

V. Conclusions

The variability of the DSD is of primary importance for radar rain-rate retrieval. A stochastic simulation framework able to reproduce realistic 2D fields of DSDs is a useful tool to investigate the influence of the variability of the DSD on many radar retrieval issues (non-uniform beam filling, attenuation, Z-R conversion to name a few). This paper presents such a simulator based on a geostatistical approach and extending previous work [7].

The proposed method is based on the assumption that the DSD can be adequately described using an exponential model with two parameters. Given the mean, the standard deviation and the (cross-)variograms of these two parameters, 2D fields

can be generated with the appropriate spatial structure. Because it is a stochastic approach, a large number of fields with identical statistical properties can be produced in a Monte Carlo framework.

However, data characterizing the spatial variability of the DSD are not available. Hence the simulator must be parameterized using available data, that is time series of DSD measurements. This is possible at the expense of the simplifying assumptions of Taylor's hypothesis and isotropy of rainfall fields. Time series of DSD measurements collected during intense Mediterranean rainfall have been used to derive the parameter values of the proposed DSD simulator.

In order to evaluate the quality of the simulated 2D DSD fields, the statistical and structural properties of the reflectivity fields derived from simulated DSD fields are compared to those of reflectivity fields observed using an operational S-band radar. Although not identical, these properties are similar enough to show that the simulated fields are realistic.

ACKNOWLEDGMENT

The authors acknowledge the financial support from the Swiss National Science Foundation (grant 200021-118057/1).

REFERENCES

[1] J. S. Marshall and W. M. Palmer, "The distribution of raindrops with size," *J. Meteor.*, vol. 5, pp. 165–166, 1948.

[2] L. J. Battan, *Radar observation of the atmosphere*. University of Chicago Press, 1973.

[3] V. N. Bringi and V. Chandrasekar, *Polarimetric doppler weather radar*. Cambridge University Press, 2001.

[4] W. F. Krajewski, R. Raghavan, and V. Chandrasekar, "Physically based simulation of radar rainfall data using a space-time rainfall model," *J. Appl. Meteor.*, vol. 32, no. 2, pp. 268–283, 1993.

[5] E. N. Anagnostou and W. F. Krajewski, "Simulation of radar reflectivity fields: Algorithm formulation and evaluation," *Water Resour. Res.*, vol. 33, no. 6, pp. 1419–1428, 1997.

[6] G. Lee, A. W. Seed, and I. Zawadzki, "Modeling the variability of drop size distributions in space and time," *J. Appl. Meteor. Climate*, vol. 46, no. 7, pp. 742–756, 2007.

[7] A. Berne and R. Uijlenhoet, "A stochastic model of range profiles of raindrop size distributions: application to radar attenuation correction," *Geophys. Res. Lett.*, vol. 32, no. 10, 2005.

[8] A. R. Jameson and A. B. Kostinski, "What is a raindrop size distribution?" *Bull. Amer. Meteor. Soc.*, vol. 82, no. 6, pp. 1169–1177, 2001.

[9] Z. S. Haddad and D. Rosenfeld, "Optimality of empirical Z-R relations," *Q. J. Roy. Meteor. Soc.*, vol. 123, no. 541, pp. 1283–1293, 1997.

[10] A. Berne and R. Uijlenhoet, "Quantification of the radar reflectivity sampling error in non-stationary rain using paired disdrometers," *Geophys. Res. Lett.*, vol. 32, no. 19, 2005.

[11] G. Vulpiani, F. Marzano, V. Chandrasekar, A. Berne, and R. Uijlenhoet, "Polarimetric weather radar retrieval of raindrop size distribution by means of a regularized artificial neural network," *IEEE T. Geosci. Remote Sens.*, vol. 44, no. 11, pp. 3265–3275, 2006.

[12] A. Berne and R. Uijlenhoet, "Path-averaged rainfall estimation using microwave links: Uncertainty due to spatial rainfall variability," *Geophys. Res. Lett.*, vol. 34, no. 7, 2007.

[13] E. Vanmarcke, *Random fields: analysis and synthesis*. MIT Press, 1983.

[14] R. G. Martin, "Comment on 'Spatial Simulation of Geologic Variables' by Zekâi Sen," *Math. Geology*, vol. 23, no. 5, pp. 789–791, 1991.

[15] J.-P. Chilès and P. Delfiner, *Geostatistics: Modeling spatial uncertainty*, ser. Probability and statistics. Wiley, 1999.

[16] E. J. Pebesma, "Multivariate geostatistics in S: the gstat package," *Comput. Geosci.*, vol. 30, no. 7, pp. 683–691, 2004.

[17] R. Uijlenhoet, H. Andrieu, G. L. Austin, E. Baltas, M. Borga, M. Brilly, I. Cluckie, J.-D. Creutin, G. Delrieu, P. Deshons, S. Fatorelli, R. J. Griffith, P. Guarnieri, D. Han, M. Mimikou, M. Monai, J. M. Porrà, D. Sempere-Torres, and D. A. Spagni, "HYDROMET Integrated Radar Experiment (HIRE): experimental setup and first results," in 29^{th} *Int. Conf. On Radar Meteorology, AMS*, Montréal, Canada, 1999, pp. 926–930.

[18] A. Berne, G. Delrieu, J.-D. Creutin, and C. Obled, "Temporal and spatial resolution of rainfall measurements required for urban hydrology," *J. Hydrol.*, vol. 299, no. 3-4, pp. 166–179, 2004.

[19] H. C. van de Hulst, *Light scattering by small particles*. Dover, 1981.